CHAPTER III

THEORY

This chapter consists of five main sections. Section 3.1 gives general information about airlift reactor. Hydrodynamics in airlift reactor is discussed in Section 3.2. Details on mass transfer in airlift reactor are described in Section 3.3. Section 3.4 discusses properties, application, and synthesis of material used in the research. Wastewater treatment application is discussed in Section 3.5.

3.1 Airlift reactor

Air-lift reactor is an important class of modified bubble columns which is one form of gas-liquid contactors for gas separation, purification, fermentation, and waste water treatment [Majeed et al., 1995]. Airlift reactor (ALR) has been recognized as an economically and technically significant reactor with its simple design and construction along with high efficiency of homogenization and intense mixing for heat and mass transfer [Jin et al., 2006].

In ALR the contents are pneumatically agitated by a stream of air or, sometimes, of other gases. The gas phase performs the dual function of aeration and agitation. In addition to agitation, the gas stream also has an important function of mediating exchange between the gas phase and the medium. Oxygen is usually transferred to the liquid flow, which depends on the geometry of the systems. The bubble column is a simple vessel where gas is injected, usually at the bottom, and random mixing of the medium is caused by the ascending bubbles. On the other hand, the major patterns of fluid circulation in ALR are determined by the reactor design. There is a channel for gas/liquid upflow (the riser) and a separate channel for the downflow (downcomer). Both channels are linked at the bottom and at the top, forming a closed loop. The circulation in ALR is induced by (i) the energy transfer from the aeration, and (ii) the net density difference between the riser and downcomer resulting from injecting gas. The gas is usually injected near the bottom of the riser.

The extent to which the gas disengages at the top section, termed the gas separator, is determined by the design and operating conditions.

ALR is particularly suitable for slow reactions since it contains recycle streams that allow for larger residence time within a small reactor volume when compared to (slurry) bubble columns and uniform distribution of the reaction components, and for multiphase (gas–liquid–solids) systems, in which high mass and heat transfer are necessary. Compared with conventional activated sludge processes, oxygen transfer rates in air-lift devices are up to 10-fold greater. ALR has been widely applied in biochemical industry, fermentation, and wastewater treatment processes [Merchuk et al., 1990; Tanthikul et al., 2004].
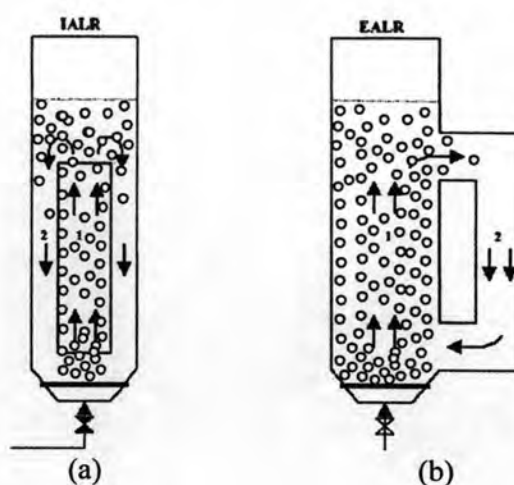
3.1.1 Type of airlift reactor

Although many geometrical differences exist in the air-lift reactors, all are characterized by two clearly differentiated sections: the riser and downcomer, which are interconnected near the top and bottom of the reactor. There are two broad categories of ALR: the internal air-lift reactor (IALR) and external air-lift reactor (EALR) according to the reactor configuration and the liquid circulation [Jin et al., 2005].

3.1.1.1 Internal-loop airlift reactor

In internal-loop types, the division section is achieved either by installation of draft tube in the cylindrical column as illustrated in Figure 3.1(a) or by a tightly fitting vertical baffle to give a split-cylinder geometry in which a part of the gas is entrained into the downcomer. Some of these types are also mounted with enlarged gas-liquid separator at the top in order to avoid gas flow into the downcomer section.

3.1.1.2 External-loop airlift reactor

External loop airlift reactor consists of two columns of liquid connected together at the top and the bottom, in which little or no gas recirculates into the downcomer. As the downcomer is, in the case, physically separated from the riser, one might assign the riser and downcomer to very different applications. For instance, riser might be used as a nitrification section (aerobic) whereas downcomer can be employed as anaerobic denitrification [Silapakul, 2002]. Figure 3.1(b) shows the schematic for the external loop airlift reactor.

Figure 3.1 Two types of airlift reactor, (a) internal loop ALR and (b) external loop
ALR1 and 2 denote riser and down comer, respectively.

All ALRs, regardless of the basic configuration (external loop or Internal
loop), comprise four distinct sections with different flow characteristics. Therefore,
mass and heat transfer will be different in each section. The four sections are:

• *Riser* Gas is injected at the base of this section. The flow is predominantly
upwards.

• *Downcomer* The downcomer is parallel to the riser and is connected to the
riser at both the bottom and at the top. The flow in the downcomer is downwards, the
driving force of this recirculation is the difference in mean density or hydrostatic
pressure between this section and the riser.

• *Base* In the vast majority of ALR designs, the bottom connection zone
between the riser and downcomer is very simple and usually not considered to
significantly affect overall reactor behavior. However, the design of this section can
influence gas holdup, liquid velocity and solid phase flow.

• *Gas separator* This section is at the top of the reactor, connecting the riser to
the downcomer, allowing liquid recirculation and gas disengagement. A design that
allows for residence time of gas in the separator to be substantially longer than the
time required by the bubbles to disengage will ensure that a minimal fraction of the
gas will circulate in the fluid through the downcomer.

Circulation of liquid and gas in ALRs is due to the difference in gas holdup between the riser and the downcomer, which creates a pressure difference, or the mixture density difference, at the bottom of the equipment that forces the fluid from the bottom of the downcomer towards the riser, generating the circulation in the ALR [Merchuk et al., 1990].

3.1.2 Advantages of airlift reactor

Airlift reactors have several advantages over another kind of reactors (bubble columns and stirred tanks), some of which are listed below [Chisti, 1989; Chisti and Moo-Young, 1987]:

- Simple design
- Absence of moving parts, stirred shaft, seals and bearings
- Ease of maintenance
- Elimination of the danger of contamination through seals
- Low power consumption
- Low capital cost
- Low shear stress
- Better defined flow pattern
- Controllable liquid circulation rate
- High mass and heat transfer
- Short mixing time
- Mild and uniform mixing
- Minimum gas velocity needed for complete suspension
- Ease of suspending solid particles (in three phases)
- Intimate contact between gas, liquid and solid phases

Despite these several advantages, mass transfer efficiencies in airlift are inferior to that obtained in stirred tanks. However, shear stress in stirred tanks is often very large, which renders this type of reactor not suitable for several types of cell cultures

Bubble columns are also appropriate for cell culture but they lack liquid circulation which results in poor mixing, particularly for the systems with high cell density, where cells tend to settle at the bottom of the system.

Because of several advantages as mentioned above, airlift reactors are finding increasing applications in various processes such as biological wastewater treatment, biochemical fermentation and cultivate cells such as algae [Loataweesup, 2002; Silapakul, 2002; Rasrikrangkrai, 2003].

3.2 Hydrodynamics in airlift reactor

The major factors that affect the performance of ALR include (1) gas characteristics (superficial gas velocity, u_{sg}; and gas bubble size); (2) physical properties of the liquid and solids (density, concentration, and viscosity); (3) operating variables (gas flow rate, R_G, dispersion height, h_D; volume of the gas–liquid separator, V_{GLS}; working volume of the liquid, V_L); (4) geometrical modifications (downcomer to riser cross-sectional area ratio, A_d/A_r; and gas distributor–sparger). Hydrodynamics such as gas holdup (ε), flow regimes, liquid circulation velocity (u_{Lc}), and volumetric mass transfer coefficient (k_La) are important parameters used in designing, operating and assessing the ALR.

To design an airlift reactor, one need to understand their hydrodynamic behavior of the system, in particular, gas holdup and liquid circulation velocity. These two parameters have been extensively studied because of their influences on transfer phenomena. The hydrodynamics behavior (gas holdup and liquid circulation velocity) in airlift reactor is discussed in this section whereas the mass transfer characteristics in the next section [Jin et al., 2006].

3.2.1 Gas holdup

The volume fraction of gas or gas holdup is as essential for the design of airlift reactor. Due to the configuration of airlift reactor that allow aeration in the riser, gas hold up in the riser is usually higher than the downcomer. This difference in gas holdups is the main cause of pressure difference, which creates liquid circulation pattern.

Gas holdup, ε, is the ratio of the volume of gas phase to the total volume of reactor (volume gas phase plus volume of liquid phase) or can be expressed as:

$$\varepsilon = \frac{V_G}{V_G + V_L} \tag{3.1}$$

where V_G is gas volume and V_L is liquid volume in reactor.

Many aspects of airlift reactor depend not only on the overall gas holdup but also on the distribution of holdups between the riser and the downcomer. The volumetric flow rate of liquid in airlift can be expressed as the product between the superficial liquid velocity and the empty column cross-sectional area:

$$Q_{Lr} = u_{Lr}A_r \tag{3.2}$$

$$Q_{Ld} = u_{Ld}A_d \tag{3.3}$$

where Q_L is the liquid flow rate, u_L is superficial liquid velocity, and A is cross-sectional area. Subscript r denotes the riser section and d denotes the downcomer section. Because all of the liquid in the downcomer must circulate back to the riser:

$$u_{Lr}A_r = u_{Ld}A_d \tag{3.4}$$

Equation 3.4 can be written in terms of the linear liquid velocities (true velocities that include the effect of bubble holdup) or

$$v_{Lr}A_r(1-\varepsilon_r) = v_{Ld}A_d(1-\varepsilon_d) \tag{3.5}$$

Where v_L is the linear liquid velocities and ε is the gas holdup. Rearrangement of Equation 3.5 leads to

$$\varepsilon_d = \frac{v_{Lr}A_r}{v_{Ld}A_d}\,\varepsilon_r - \left(\frac{v_{Lr}A_r}{v_{Ld}A_d} - 1\right) \tag{3.6}$$

Equation 3.6 is a rather common expression for the relationship between riser and the downcomer gas holdups. A general form of Equation 3.6 is:

$$\varepsilon_d = \alpha\varepsilon_r - \beta \qquad (3.7)$$

where

$$\alpha = \frac{v_{Lr}A_r}{v_{Ld}A_d} \qquad (3.8)$$

and

$$\varepsilon_d = \alpha\varepsilon_r - \beta \qquad (3.9)$$

Gas holdup can be an indicator for the mean residence time of the gas phase. It also affects the liquid circulation velocity and the mixing behavior. Increasing superficial gas velocity (u_{sg}) increases the gas holdup. Changes in the downcomer to riser cross-sectional area ratio (A_d/A_r) will alter the liquid and gas residence times in each part of the reactor. The gas holdup decreases with an increase in A_d/A_r. Because increasing A_d/A_r enhances the liquid circulation velocity and shortens the time that the bubbles spend in riser, gas holdup in riser decreases.

3.2.2 Liquid velocity

As stated earlier, the difference in gas holdup is the main reason that induces the liquid circulation in airlift reactor. Liquid flows upward in the riser and downward in the downcomer where circulation velocity (u_{Lc}) is

$$\bar{u}_{Lc} = \frac{x_c}{t_c} \qquad (3.10)$$

Where x_c is circulation length and t_c is an average time for one complete recirculation.

To find the relationship between the riser and downcomer liquid velocities, the continuity equation is formulated:

$$u_{Lr}A_r = u_{Ld}A_d \qquad (3.11)$$

The superficial liquid velocity is different from the true linear velocity because of the existence of bubble in liquid phase. The linear liquid velocity, v_L, and the superficial liquid velocity are related as follows:

$$v_{Lr} = \frac{u_{Lr}}{1 - \varepsilon_r} \tag{3.12}$$

and

$$v_{Ld} = \frac{u_{Ld}}{1 - \varepsilon_d} \tag{3.13}$$

The increasing in the superficial gas velocity (u_{sg}) increases the liquid circulation velocity (v_L). The liquid circulation velocity increases with an increase in the downcomer to riser cross-sectional area ratio (A_d/A_r). Generally, a decrease in A_r rendered the liquid in riser to move faster and led to an increase in liquid circulation [Al-Masry and Abasaeed, 1998].

3.3 Mass transfer in airlift reactor

One of the most important factors for the operation of bioreactor is the gas-liquid mass transfer. However, the level of dissolved oxygen in water is always limited by thermodynamics where solubility of oxygen in water is only around 7 ppm at ambient condition. The rate at which oxygen is dissolved into the water is therefore an important key step. Therefore we need to know the behavior of the system in transferring gas between the two phases.

The overall volumetric mass transfer coefficient (or k_La) is a combination of two variables, i.e. k_L and a. k_L is mass transfer coefficient and a is surface area of transferring. The determination of each of these parameters requires a tedious experimental work on the measurement of bubble size distribution and this is often not practical in large scale system. A more conventional method of determining the rate of gas-liquid mass transfer is to find the product of the two quantities, k_La.

To determine this parameter, the method based on a dynamic approach of oxygen is employed. Oxygen balance performed across an aerated bioreactor is formulated:

$$\frac{dC_L}{dt} = k_La(C_L^* - C_L) \tag{3.14}$$

where C_L is the dissolved oxygen concentration, C_L^* is the dissolved oxygen concentration in equilibrium with partial pressure of oxygen in the air, and k_La is the volumetric oxygen transfer coefficient.

The Increasing of the superficial gas velocity (u_{sg}) increases the mass transfer coefficient (k_La). In contrast, when A_d/A_r ratio increases, mass transfer decreases. When A_r decreases, bubbles can move faster because of large velocity of liquid, hence transferring time is poor [Al-Masry and Abasaeed, 1998].

3.4 Titanium dioxide

This section discusses properties and applications of titanium dioxide. This material was employed as the catalyst for photocatalytic degradation of organic dyes in this study.

3.4.1 Physical and Chemical properties [Othmer, 1991; Fujishima et al., 1999]

Titanium dioxide may take on any of the following three crystal structures: anatase, which tends to be more stable at low temperature; brookite, which is usually found only in minerals; and rutile, which tends to be more stable at higher temperatures. Anatase generally shows a higher photocatalytic activity than the other types of titanium dioxide. Comparison of some physical properties of anatase, brookite and rutile is listed in Table 3.1.

Although anatase and rutile are both tetragonal, they are not isomorphous. Anatase occurs usually in near-regular octahedral structure and rutile forms slender prismatic crystal, which are frequently twinned. Rutile is the thermally stable form and is one of the two most important ores of titanium.

The three forms of titanium (IV) oxide have been prepared in laboratories but only rutile, the thermally stable form, has been obtained in the form of transparent large single crystal. The transformation from anatase to rutile is accompanied by the

evolution of ca. 12.6 kJ/mol (3.01 kcal/mol), but the rate of transformation is greatly affected by temperature and the presence of other substances, which may either catalyze or inhibit the reaction. The lowest temperature at which transformation from anatase to rutile takes place at a measurable rate is around 700°C, but this is not a transition temperature. The change is not reversible since ΔG for the change from anatase to rutile is always negative.

Table 3.1 Comparison of rutile, brookite and anatase. [Othmer, 1991 and Fujishima et al., 1999].

Properties	Anatase	Brookite	Rutile
Crystal structure	Tetragonal	Orthorhombic	Tetragonal
Optical	Uniaxial, negative	Biaxial, positive	Uniaxial, negative
Density, g/cm^3	3.9	4.0	4.23
Harness, Mohs scale	$5^1/_2 - 6$	$5^1/_2 - 6$	$7 - 7^1/_2$
Unit cell Dimension, nm	$D_4a^{19}.4TiO_2$	$D_2h^{15}.8TiO_2$	$D_4h^{12}.3TiO_2$
a	0.3758	0.9166	0.4584
b	-	0.5436	-
c	0.9514	0.5135	2.953
Refractive index	2.52	-	2.52
Permittivity	31	-	114
Melting point	changes to rutile at high temperature	-	1858°C

Brookite has been produced by heating amorphous titanium (IV) oxide, which is prepared from an alkyl titanate or sodium titanate, with sodium or potassium hydroxide in an autoclave at 200 to 600 °C for several days. The important

commercial forms of titanium (IV) oxide are anatase and rutile, and they can readily be distinguished by X-ray diffractometry.
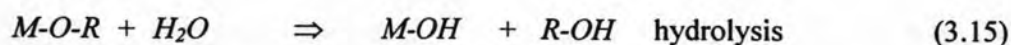
Since both anatase and rutile are tetragonal, both of them are anisotropic. Their physical properties, e.g., refractive index, vary according to the direction relative to the crystal axes. In most applications of these substances, the distinction between crystallographic direction is lost because of the random orientation of large numbers of small particles, and only average values of the properties are significant.

Measurement of physical properties, in which the crystallographic directions are taken into account, may be made for both natural and synthetic rutile, natural anatase crystals, and natural brookite crystals. Measurements of the refractive index of titanium (IV) oxide must be made by using a crystal that is suitably orientated with respect to the crystallographic axis as a prism in a spectrometer. Crystals of suitable size of all three modifications occur naturally and have been studied. However, rutile is the only form that can be obtained in large artificial crystals from melts. The refractive index of rutile is 2.75. The dielectric constant of rutile varies with direction in the crystal and any variation from the stoichiometric formula, TiO_2. An average value for rutile in powder form is 114. The dielectric constant of anatase powder is 48.

Titanium (IV) oxide is thermally stable (mp 1855 °C) and very resistant to chemical attack. When it is heated strongly under vacuum, there is a slight loss of oxygen corresponding to a change in composition to $TiO_{1.97}$. The product is dark blue but reverts to the original white color when it is heated in air.

3.4.2 Preparation of Titanium dioxide via a sol-gel method [Fu et al., 1996; Su et al., 2004]

Sol-gel process occurs in liquid solution of organometallic precursors such as tetraethyl orthosilicate, zirconium propoxide and titanium isopropoxide, which, by means of hydrolysis and condensation reaction, lead to the formation of sol.

$$M\text{-}O\text{-}R + H_2O \quad \Rightarrow \quad M\text{-}OH + R\text{-}OH \quad \text{hydrolysis} \quad (3.15)$$

$$M\text{-}O\text{-}H + HO\text{-}M \quad \Rightarrow \quad M\text{-}O\text{-}M + H_2O \quad \text{water condensation} \quad (3.16)$$

$$M\text{-}O\text{-}R + HO\text{-}M \quad \Rightarrow \quad M\text{-}O\text{-}M + R\text{-}OH \quad \text{alcohol condensation} \quad (3.17)$$

A typical example of a sol-gel method is the addition of metal alkoxides to water. The alkoxides are hydrolyzed, giving the oxide as a colloidal product.

The sol is made of solid particles of a diameter of few hundred nanometers suspending in a liquid phase. After that, the particles condense into gel, in which solid macromolecules are immersed in a liquid phase. Drying the gel at low temperature (25-100°C), produces porous solid matrices or xerogels. To obtain a final product, the gel is heated. This heat treatment serves several purposes, i.e., to remove solvent, to decompose anions such as alkoxides or carbonates to give oxides, to rearrange of the structure of the solid, and to allow crystallization to occur.

Using the sol-gel method, one can easily control a stoichiometry of solid solution and a homogeneous distribution of nanoparticles and metal oxides. In addition, the advantages are that the metal oxides are prepared easily at room temperature and high purity can be obtained

3.4.3 Applications of titanium dioxide

Titanium dioxide is one of the most basic materials in our daily life. Titanium dioxide has been used in paints, plastics, paper, inks, fibers, cosmetics, sunscreens and foodstuffs.

Naturally, the type of titanium dioxide that is used as a pigment is different from that used as a photocatalyst. Various applications in which research and development activities involving titanium dioxide have been investigated, such as fog-proof, anti-bacterial, anti-viral, fungicidal, anti-soiling, self-cleaning, deodorizing, air purification, anti-cancer, water treatment and water purification.

3.5 Titanium dioxide with wastewater treatment

Among the new oxidation methods or advanced oxidation processes (AOP), heterogeneous photocatalysis appears to be an emerging destructive technology leading to total mineralization of most organic pollutants.

Titanium dioxide, particularly in the anatase form, is a photocatalyst under ultraviolet light. The strong oxidative potential of the positive holes oxidizes water to create hydroxyl radicals. It can also oxidize oxygen or organic materials directly.

TiO_2 is appropriate as an agent in remediation of wastewater due to several factors. First the process occurs under ambient conditions. There is no formation of photocyclized intermediate products, which are produced from direct photolysis techniques. Oxidation of the substrates result in CO_2 as a products. The photocatalyst is inexpensive and has a high turnover. TiO_2 can be supported on suitable reactor substrates. The process offers great potential as an industrial technology to detoxify wastewaters. Upon illumination of light possessing greater energy than the band gap on TiO_2, it can initiate decomposition and complete breakdown of organic compounds.

The presence of both UV radiation to activate the titanium dioxide particles and visible radiation to excite the dye molecules allows for the dye to be photodegraded by both a photocatalytic and photosensitization process. When irradiated at a wavelength less than 380 nm, electrons in titanium dioxide are excited from the valence band to the conduction band producing a positively charged hole in the catalyst. The organic matter is oxidized at the catalyst surface and in the solution by any of the following routes: hydroxyl radicals, superoxide radicals or direct oxidation by positive holes. The reaction scheme is as followed:

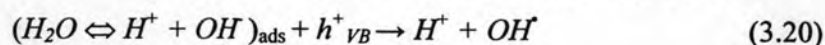1. Absorption of photons with sufficient energy ($hv \geq E_G = 3.2$ eV) by titania

$$TiO_2 + hv \rightarrow e^-_{CB} + h^+_{VB} \qquad (3.18)$$

2. Oxygen ionosorption (first step of oxygen reduction; oxygen's oxidation degree passes from 0 to $-1/2$)

$$(O_2)_{ads} + e^-_{CB} \rightarrow \bullet O_2^- \tag{3.19}$$

3. Neutralization of OH^- groups by photoholes which produces $OH^{\bullet}$ radicals

$$(H_2O \Leftrightarrow H^+ + OH^-)_{ads} + h^+_{VB} \rightarrow H^+ + OH^{\bullet} \tag{3.20}$$

4. Neutralization of $\bullet O_2^-$ by protons

$$\bullet O_2^- + H^+ \rightarrow \bullet HO_2 \tag{3.21}$$

5. Transient hydrogen peroxide formation and dismutation of oxygen

$$2\bullet HO_2 \rightarrow H_2O_2 + O_2 \tag{3.22}$$

6. Decomposition of H_2O_2 and second reduction of oxygen

$$H_2O_2 + e^- \rightarrow \bullet OH + OH^- \tag{3.23}$$

7. Oxidation of the organic reactant via successive attacks by $OH^{\bullet}$ radicals

$$R + \bullet OH \rightarrow \bullet R' + H_2O \tag{3.24}$$

8. Direct oxidation by reaction with holes

$$R + h^+ \rightarrow \bullet R^+ \rightarrow degradation\ products \tag{3.25}$$

However, photodegradation of dyes over TiO_2 may also occur by photosensitization. In this process the colored compound absorb radiation in the visible range to yield an excited state of the dye, dye*. The dye transfers an electron to the semiconductor particle to produce a conduction band radical and a dye radical cation, which, in turn, reduces molecular oxygen to form a superoxide anion. Eventually, the dye cation radical reacts with molecular oxygen or with an oxygenated radical species to yield a mineralized product.

$$dye + h\nu \longrightarrow dye^* \tag{3.26}$$

$$dye^* + TiO_2 \longrightarrow dye^+ + TiO_2\ (e^-_{CB}) \tag{3.27}$$

$$\bullet O_2^- + e^-_{CB} + 2H^+ \longrightarrow H_2O_2 \tag{3.28}$$

$$dye^+ + O_2\ (and\ /\ or\ O_2^-\ and\ /\ or\ \bullet OH) \longrightarrow mineralized\ products \tag{3.29}$$